Changes in Usage of an Indoor Public Space: Analysis of One Year of Person Tracking

ARTICLE *in* IEEE TRANSACTIONS ON HUMAN-MACHINE SYSTEMS · JANUARY 2014

Impact Factor: 1.98 · DOI: 10.1109/THMS.2014.2374172

2 AUTHORS:

Drazen Brscic

Advanced Telecommunications Research Ins…

28 PUBLICATIONS **151** CITATIONS

SEE PROFILE

Takayuki Kanda

Advanced Telecommunications Research Ins…

263 PUBLICATIONS **4,260** CITATIONS

SEE PROFILE

Changes in Usage of an Indoor Public Space: Analysis of One Year of Person Tracking

Dražen Brščić, *Member, IEEE,* and Takayuki Kanda, *Member, IEEE*

***Abstract*—Knowledge about space usage from variables such as density and walking speed could support a variety of service applications. However there is not much knowledge on how the usage of space changes during extended periods of time and what affects the changes. We have installed a person tracking system in a large area of a shopping center, and collected pedestrian data over a year. In this paper we analyze the collected data to find the changes in pedestrian density and speed, percentage of children, and pedestrian trajectories. The changes from day to day, as well as during the day are examined and a number of factors that affect them are identified. This is in turn used in the prediction of the state of the space using a Gaussian process model.**

Fig. 1. Public space at different times of year (on Sunday, around 14:00)—are there differences in the usage of space?

I. Introduction

ANALYSIS and modeling of human usage of public spaces is very important in a wide range of applications. For example, knowledge about the motion and behavior inside a certain environment can be used to improve the services that are provided.

Modeling the microscopic pedestrian behavior (behavior of individual pedestrians, e.g. how pedestrians move towards a goal while avoiding each other, and how they form groups) supports simulating and predicting the motion of multiple pedestrians inside a space. Common applications based on microscopic pedestrian behavior models include the assessment of the accessibility [1], safety of spaces during emergency situations [2], [3], and automatic detection of unusual behavior [4], [5].

The use of models of person motion and space usage is also becoming common in robotics, especially for social robots. For example, motion patterns learned from observations of humans can be used to make the navigation among people more effective [6], [7]. In addition, knowledge of people's behavior can support devising ways for robots to approach people [8], find appropriate places to offer services [9] or chose a place for waiting [10].

It is not clear if models of behavior based on data collected at one specific point of time apply at some different time. Usage of space can be dependent on the time when it is observed. This suggests that for the prediction or simulation of the complete state of an environment at a certain instant, in addition to a microscopic behavior model, it may be necessary to specify the conditions for the model at that instant. The conditions include variables such as the number of people in the space, and their flow and preferred velocities. These variables and their dynamics can jointly be called the macroscopic pedestrian behavior. To reproduce the pedestrian state during extended periods it may be necessary to account for changes in macroscopic behavior variables.

This work addresses how does the macroscopic behavior in a public space change in time, both during a single day and over longer periods; what factors affect the changes; and can the state of the space be predicted based on available knowledge of the factors that cause the change. For instance, when using robots as shop keepers, these answers could inform the appropriate number of robots required, robot battery charging schedules, or robot placement, as in [9].

The study of long-term macroscopic behavior in public spaces has been limited by the ability to detect and continuously track people in a wide area and for a long time. We installed multiple 3-D range sensors in a shopping center and developed a tracking system to collect the position data for all visitors. We used this system to save tracking data twice every week, during one year. Here we analyze the data, specifically focusing on the changes in the macroscopic behavior that occurred during the observation period.

II. Related Work

A. Long-term Collection of Pedestrian Data

Different ways for obtaining pedestrian trajectories inside a space have been proposed [11]. The traditional approach is through surveys or manual marking of the route of a person on a map [12]. Another alternative is manual annotation of positions in videos. For long-term pedestrian position data, these methods are too labor intensive.

For collecting large amounts of pedestrian data wearable sensors have been used, such as RFID or WiFi tags. For example Larson et al. [13] used RFID tags to track people

Manuscript received ... This work was supported by the Japan Science and Technology Agency (JST), Core Research for Evolutional Science and Technology (CREST) program.

D. Brščić and T. Kanda are with the Advanced Telecommunication Research Institute International (ATR), 2-2-2 Hikaridai, Seika-cho, Soraku-gun, Kyoto 619-0288, Japan; (e-mail: drazen@atr.jp; kanda@atr.jp).

in a supermarket. In [14] RFID tags were used in a museum for a period of 25 days. However, requiring people to wear sensors is often impractical and can also affect behavior.

Another approach is using sensors installed in the environment. In [15], an automated pedestrian counter was installed on a street for one year and the influence of weather on the number of pedestrians was studied. However, compared to tracking, counting only provides pedestrian information limited to a particular position in the space.

Standard cameras have often been used for tracking. In [16]–[18], authors analyzed pedestrian trajectories in open public spaces. Publicly available pedestrian tracking datasets that span multiple days include the MIT dataset [18] and the BIWI dataset [19]. Considering the large number of surveillance cameras installed in many public areas, there is an expectation of the use of standard cameras for tracking [4]. Nevertheless, robust and reliable tracking in public spaces using cameras remains limited due to occlusions, scene variability, and other factors [11].

Tracking systems that use laser range finders [5], [20], [21] or 3-D range sensors [22], [23] (including also the system in [24] used in this work) are much less affected by these problems. In particular, they are not as strongly influenced by lighting conditions and objects in the environments, which can change significantly during the day and at different times of the year.

The prior work on pedestrian tracking generally focused on a small area over a limited period. One exception appears in [25], where 3-D range sensors were used for tracking people inside a train station for several months; however only 4 days of data are analyzed.

B. Modeling and Simulation of Pedestrian Behavior

Modeling of pedestrian motion has received much interest, especially the study of pedestrian dynamics during evacuation and panic situations (see [2] for a review). One popular model is the social-force model [26], and improved variants of the basic model that better describe dynamics in less crowded public environments appear in [27], [28].

While these works model pedestrian behavior on a microscopic level by describing avoidance behavior between pedestrians, others address how people traverse the environment [17], [29], [30]. In an example from the human-robot interaction field, Bennewitz et al. [6] learned people's trajectories and predicted their future motion in order to help a robot effectively avoid people.

These models allow one to simulate pedestrian behavior inside an environment to support evaluation of the usage of space, without long-term collection of real pedestrian data. For example, in [1] the authors use simulation of pedestrian behavior in order to assess the design of a train station. In [9] we used a pedestrian simulator to reproduce crowding effects around a social robot, and to support robot motion planning.

In this paper we are not interested in the modeling or simulation of the behavior of each single person. Instead we wish to study the macroscopic behavior of the crowd, i.e. the changes in pedestrian statistics that happen in the environment over extended periods of time.

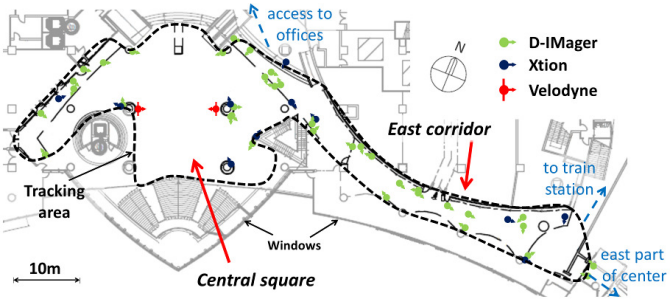

Fig. 2. Tracking area and sensor setup in ATC shopping mall. The dashed line shows the border of the area covered by the sensors.

III. Data Collection Methods

A. Environment

The data were collected at the Asia & Pacific Trade Center (ATC) in Osaka, Japan. ATC includes a shopping center and office buildings. Pedestrians include office workers and occasional visitors like shoppers and travelers. A map of the considered area and the sensor arrangement are shown in Fig. 2.

In the west part of the covered area there is a large square, which connects to a long corridor to the east. The corridor leads to the train station and to the rest of the shopping center. Along the north side of the corridor there are several shops. Going north from the square it is possible to access escalators and elevators which lead to shops, offices and parking lots. Additionally, the short corridor to the west of the square leads to a ferry terminal, a convenience store and other elevators.

Preliminary observations identified two patterns of space usage. During the week, there were fewer people and many appeared to work in the center. Most would transverse the observed area without stopping, with the main flow through the east corridor. On the weekends there were more people. The largest flow was in the east corridor. In the central square, which was almost empty during the week, there were more people on the benches. In addition, more customers visited the shops in the east corridor.

B. Sensor Setup and Tracking Method

The tracking method and the sensor setup are described in [24] and summarized here. The approximately 900 m^2 area was covered with a combination of different 3-D range sensor types. For coverage we used a combination of time-of-flight cameras (Panasonic D-IMager), structured light cameras (Asus Xtion) and rotating laser scanners from Velodyne.

The sensors were mounted overhead at approximately 4m height (8m for rotating laser scanners). Due to the high mounting the obtained measurements were noisy and there were missing values. For tracking we used a heuristic method robust to the imperfections in the measurements. The basic principle of the method is sketched in Fig. 3. First, from the 3-D range scan obtained from a sensor all static parts are removed, leaving only the points belonging to moving objects, i.e. people. These points are then clustered such that each cluster corresponds to a single person. Next, the clusters are

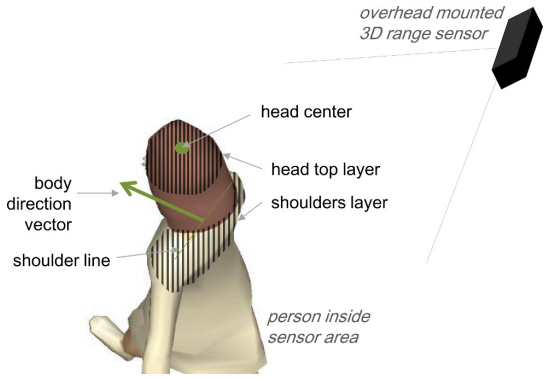

Fig. 3. Tracking method.

divided vertically into layers of fixed height and the layers belonging to the top of the head and shoulder area are extracted (shown as shaded regions in Fig. 3). The mean value of the points in the head layer provides the head center, which defines the position and height of the person. The body orientation is extracted from the shoulder layer as the vector perpendicular to the line connecting both shoulders.

These calculations are done separately for each sensor. Then the single-sensor estimates of person position, height and body angle are combined using a particle filter to obtain smooth and continuous tracking in the whole area.

C. Tracking Performance

We evaluated the tracking system performance using the CLEAR MOT metrics [31]. The obtained multiple object tracking accuracy (MOTA) was 98.6% on weekdays and 93.2% on the weekend. Considering the size of the area this result is very good, with continuous tracking most of the time, and a low number of false positives and misses. See [24] for more tracking results.

We look at the tracking failure cases in more detail in order to understand how they might affect the analysis. The most common issue concerns the errors in the identity of a person. These can be either the assignment of a different ID to a person due to a temporary tracking loss, or a switch of IDs between people, which can occur when two pedestrians are very close. On a manually labeled sample containing both Wednesday and Sunday data the ratio of pedestrians for whom the ID errors occurred at some point was 17%. For 7.1% of the people the ID changed during tracking, whereas for 11.8 % of the people there was an ID switch to a different person (this chiefly happened between people in the same group). As a result of ID changes, part of the obtained trajectories were split in two parts. ID switching sometimes resulted in distorted trajectories, but as it mainly happened inside groups, generally the changes in shape of the affected trajectories were not large.

These changes in single trajectories due to ID related errors have an effect on the analysis of trajectories, which is presented in Section V. The rest of the analysis does not look at single trajectories, so the effect of these errors is small.

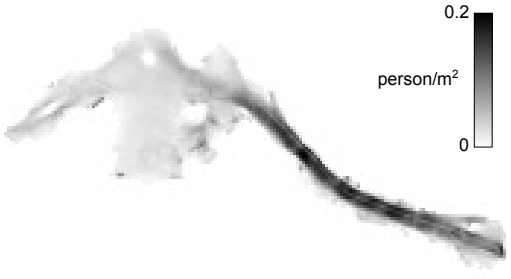

(a) Average density.

(b) Average speed.

Fig. 4. Distribution of (a) average density and (b) average speeds. (Note: stripes in the corridor are artifacts of the tracking system at the sensor boundaries.)

D. Collected Data

In the following analysis we use the data collected from the beginning of October 2012 until the end of September 2013. During this period we saved the data twice every week, except around New Year. The days of saving were fixed: Wednesday was chosen as a representative of a weekday with a relatively small number of visitors and Sunday was selected as a crowded weekend day. In the analysis below we use data from 45 Wednesdays and 42 Sundays for which tracking data for the entire day were collected. The data were saved from 10:00 to 20:00.

To analyze the spatial and temporal changes, we divided the space into equally spaced grid cells of size 0.5x0.5m. For each cell we counted the number of people passing through in a certain time interval, their walking speed and height. This information allowed us to extract variables such as density, speed, and the percentage of children.

IV. Analysis of the Data

A. Usage of Space

Fig. 4(a) shows a map of the average person density in the space. The most dense area is the east corridor. As the corridor connects this part of the shopping center to the train station and the rest of the center, a large number of people pass through it. The flow splits once it reaches the west end of the corridor, with many exiting the area to the north of the square and the rest entering the square or crossing it and proceeding to the west corridor. Fig. 4(b) indicates the parts of the space where people tend to walk and where they stay for longer periods or walk more slowly.

Using density and speed as features, it is possible to partition the total area into parts where similar conditions are

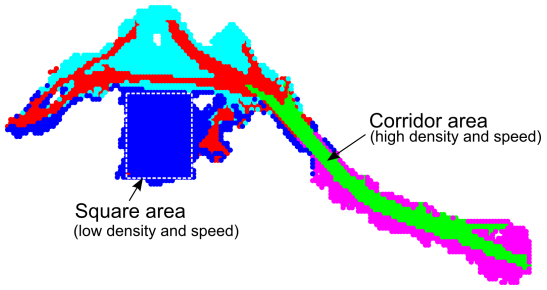

Fig. 5. Space partitioning using k-means (k=5). Two sub-areas that are considered in the analysis are also noted: corridor (in green), and square (inside white dashed rectangle).

expected. For each grid cell we defined a feature vector which consists of the density and speed values (from Fig. 4), and the (x, y) position coordinates of the cell for grouping spatially close parts together. We then run the k-means clustering on the feature set. The partitioning obtained using k=5 is shown in Fig. 5. This partitioning allows us to define two sub-areas used in the analysis below. One is the *corridor area*, which extends through the east corridor (green partition in Fig. 5). This is an area with high density and velocities. Another interesting part of the space is the *square area* for which we use the central part of the blue partition, corresponding to the central and south part of the square. Both the density and velocities in this area are low.

Notice how the green and red partitions (i.e. areas of high velocity and relatively high person density) outline the main routes in the area: the corridors on the east and west, and the top part of the square which is traversed either to go from one corridor to the other or to move between the corridors and the space to the north out of the observed area.

An animation of the variations during the day and during the year can be seen in the video accompanying the paper.

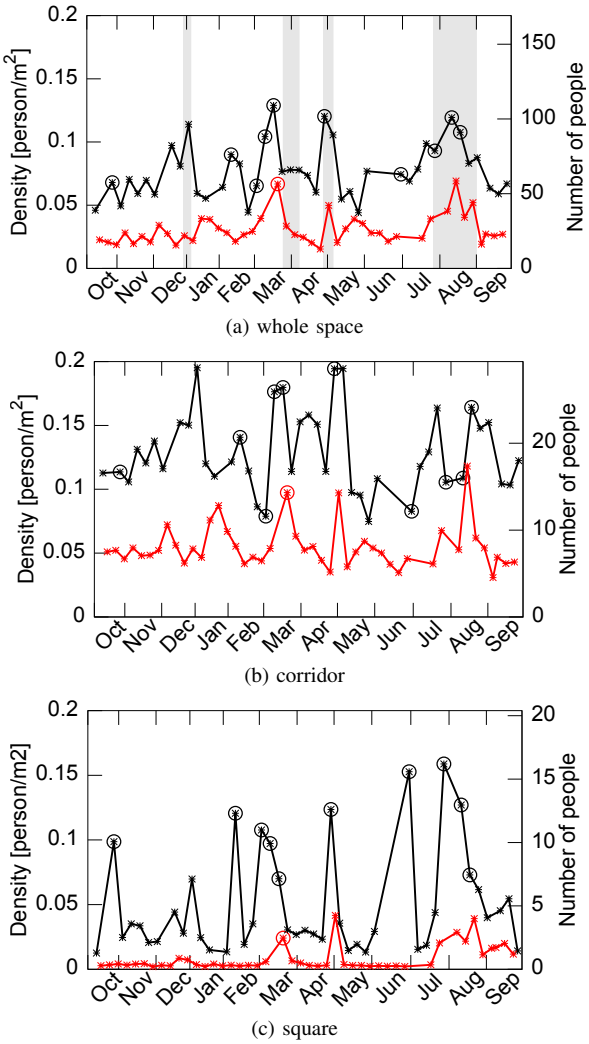

(a) whole space

(b) corridor

(c) square

Fig. 6. Average daily densities and number of people throughout the observation period in (a) whole space, (b) corridor, and (c) square (black = Sunday, red = Wednesday).

B. Variations During the Observation Period

We analyzed the changes that occurred from day to day during the observation period. The average densities for each day for the whole observed space are shown in Fig. 6(a).

There is a significant difference between the densities on Sunday and Wednesday (Welch t-test: t=12.6, $p<0.001$). The number of people on Sundays is also higher and has more variability than on Wednesdays (Sunday: mean 64.0, s.d. 22.4; Wednesday: mean 24.3, s.d. 6.6).

Sunday events, noted with circles in Fig. 6, appear to cause an increase in the number of people. They include various organized happenings for visitors, when sometimes a stage, stalls or other attractions are set up inside the square. The events which were observed during the observation period were very different from each other, in their duration, the number and type of persons they attract, the facilities brought to the area, and their arrangement, so some, for example the single event in October, seem to have had a smaller effect on the whole area density. As we could not predict how many people will a certain event attract, we treated all events in the same way.

Another possible influence on the density are vacation periods: around Christmas and New Year, spring school break, the "Golden week" in the beginning of May when there are several national holidays in Japan, and summer vacations. These periods correspond to school holidays, when the number of school children as well as their families that visit the center increases. The vacation periods are noted as grayed areas in Fig. 6(a).

The Wednesday data also show the influence of vacation periods, although it seems that the winter and spring breaks did not have a large effect. Another distinctive peak in the Wednesday data is the Vernal Equinox Day on March 20 (circled in the graph), a holiday in Japan.

The variation of density in the corridor area in Fig. 6(b) follows a similar pattern to that of the whole space density, albeit with higher values (in average 1.75 times higher). On the other hand, the square data show a different pattern, Fig. 6(c). Since the square area is not on the main route through the space (see Figs. 4 and 5), a small number of people traverse it during the week. On Sundays (as well as on Wednesdays during summer vacations) there are more people in the square.

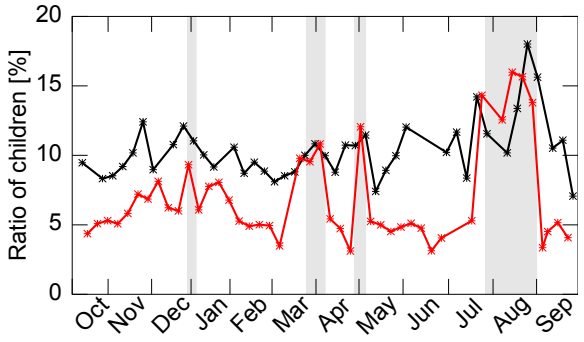

Fig. 7. Percentage of tracked objects of lower height in corridor during the year (black = Sunday, red = Wednesday).

There are more visitors and some of them use this area to wait for someone or to relax. As the events are chiefly organized in this area, the highest density values correspond to days with events.

We analyzed the percentage of people of low height, using a 1.4 m threshold to consider children in the space (1.4 m is the average height of 10 year old Japanese children). Since our tracking system does not directly distinguish between children and other low persons or objects these data can be influenced by objects such as baby strollers, wheelchairs, tables and chairs, or people sitting during events. Therefore we only consider the corridor area, where we hope that the influence of low objects is relatively small. Analysis on an one-hour sample of the Sunday data showed that approximately 64% of tracked objects in the corridor that were below the threshold actually corresponded to children, and around 21% to baby strollers, whereas the rest came from people in wheelchairs or carts used by workers.

The result appears in Fig. 7. There are in general more children on Sundays than on Wednesdays, as also confirmed in our personal experience. The percentage on Sundays appears to increase during the summer break. The Wednesday data indicate an increase during vacation periods as well as for the holiday on March 20.

We did not observe patterns for velocities or other variables during the year.

C. Variations During a Single Day

To analyze variations during a single day, we divided the time of day into 10-minute intervals and calculated the average density for each time interval. The values for the intervals were averaged for all the days, separately for Sundays and Wednesdays, see Fig. 8.

The density of the whole space (Fig. 8(a)) increases during the morning, peaks during the day and finally decreases in the evening. This pattern of change of the density during the day is similar for both Sunday and Wednesday. Wednesdays shows little variation during the year, as the relatively small standard error also illustrates.

The corridor density variation during the day is larger in scale than the whole space density, Fig. 8(b). Fig. 8(c) shows that, while being more empty during the week, the square is used more on Sunday. The comparatively large standard error

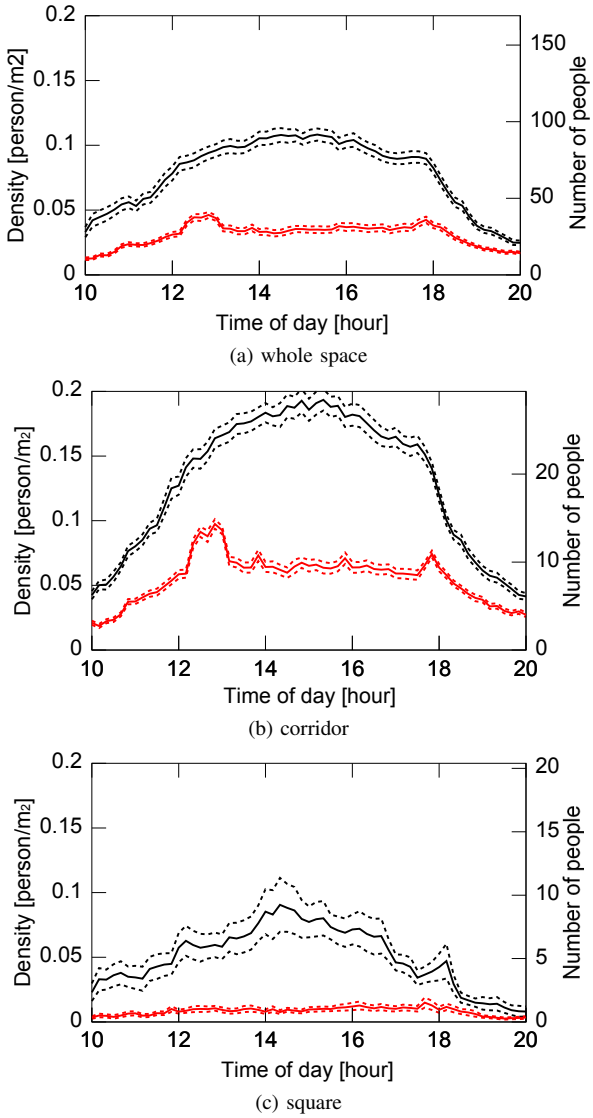

Fig. 8. Average density during the day in (a) whole space, (b) corridor, and (c) square (black = Sunday, red = Wednesday). The dashed lines represent the ± 1 standard error.

in the square data for Sunday is due to the large variation in the density from day to day, as confirmed in Fig. 6(c).

The Wednesday data indicates two peaks between 12:00 and 13:00 and around 18:00. These appear to correspond to the workers "rush hours", i.e. the lunch hour and end of work. The increased number of people in the space can be explained by the workers passing through the area. These peaks are not visible in the Sunday data, which might be explained by the relatively smaller number of workers on weekend.

We analyzed the average walking speed throughout the day, in particular for the corridor area, as shown in Fig. 9. The speed is higher in the morning. Lower values during the day may be due to the increased crowdedness of the corridor. The average speed on Sundays is smaller than on weekdays. Two peaks occur on Wednesday during the workers' rush hours, suggesting that the workers typically walk faster.

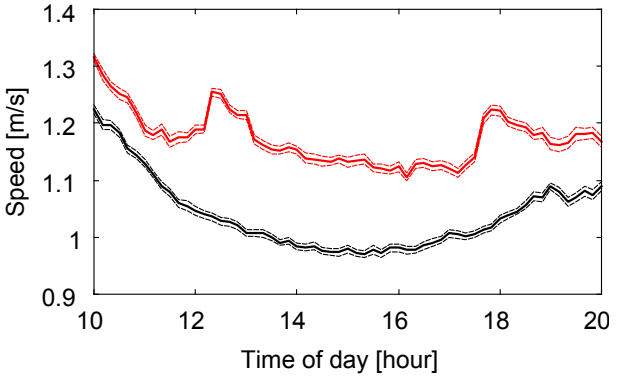

Fig. 9. Average speed in corridor (black = Sunday, red = Wednesday), with ± 1 standard error shown with dashed lines.

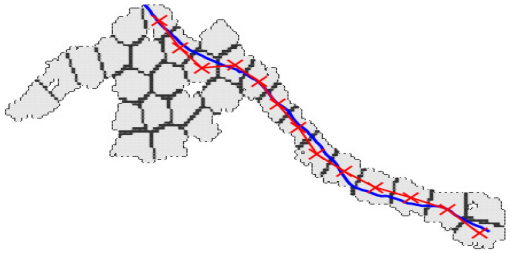

Fig. 10. Division of space into regions for trajectory coding.

V. Analysis of Trajectories

Trajectories only consider the route that the pedestrians take, without regard to their walking pace, so they provide a different perspective on the space usage. We classified the trajectories depending on their shape, and then examined the change of the distribution of the classes.

A. Trajectory Classification Method

We used an approximate trajectory classification method. Instead of working with the full trajectory information, we used a compressed representation. We divided the space into 0.5x0.5m cells, and ran a k-means algorithm on the grid centers. We obtained a Voronoi tessellation of the space, Fig. 10, where the area is divided into regions of approximately equal sizes. For each person we noted the order in which she/he went from one region to another, as shown in Fig. 10 for one sample trajectory. For the classification we use the obtained sequence of regions instead of the full person's trajectory.

To cluster the sequences representing the trajectories, we defined a distance measure for the sequences, where the distance between two sequences is defined as the sum of distances between the matching points, which is given by the Euclidean distance of the corresponding region centers. The points are matched in order, but we also allow for skipping of one point to compensate for the fact that very close trajectories might pass through different regions, thereby giving a slightly different sequence. If sequences are of different length, the distances of the not matched points to the closest point in the short sequence are also added.

Finally we cluster the sequences using k-medoids, a clustering method similar to k-means, where the center of a cluster is given by one of the sequences (the *medoid*) instead of the mean (the mean is not defined in this case). Specifically, we use the Partitioning Around Medoids algorithm [32].

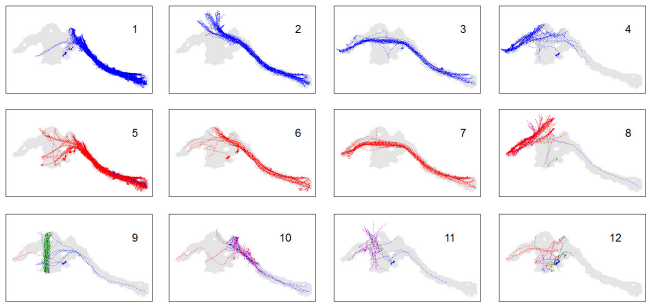

Fig. 11. Classes of trajectories obtained after clustering. Colors show the main moving direction: blue = west-east, red = east-west, green = north-south, magenta = south-north.

B. Classification Results

We first extracted clusters from a sample of trajectories and after that, classified the rest of the trajectories using the obtained clusters. The trajectory sample consisted of 1-hour periods from 3 days (2 Sundays, 1 Wednesday). After discarding short sequences with less than 4 elements we encoded the remaining trajectories into sequences.

We tested different numbers of clusters and used 12. In Fig. 11, the first row contains four main groups of trajectories going from east to west with differing start and end points: number 1 going through the corridor and exiting at the west end of the corridor, 2 proceeding further across the square and then exiting to the north, 3 going even further until the west end of the area, and 4 just passing through the short west corridor. The clusters in the second row are similar, but for trajectories going in the opposite direction. Comparing the first 8 clusters with Figs. 4 and 5, they correspond with the main routes through the space.

The rest of the clusters mostly contain activities on and around the square. Clusters 9 and (less clearly) 11 capture one more distinctive trajectory pattern—people moving between the south and north sides of the square. Going south from the square area it is possible to move outside into an open space between the shopping center and the sea. This was used mainly by visitors on Sundays. This represented only a minor flow and it is not noticeable in the average density and velocity in Fig. 4.

The obtained division into clusters was used on the rest of the data to classify all trajectories into one of the clusters, by associating each trajectory to the closest medoid. This information on the trajectory classes is analyzed next.

We first looked at the distribution of the trajectory classes (note that this frequency distribution might have been partially influenced by the splitting of trajectories due to ID changes, discussed in Section III-C). Figure 12 shows the average values of the relative frequencies for each class. Trajectories where people only stay in the tracking area while passing through the east corridor, entering on one end and exiting at the

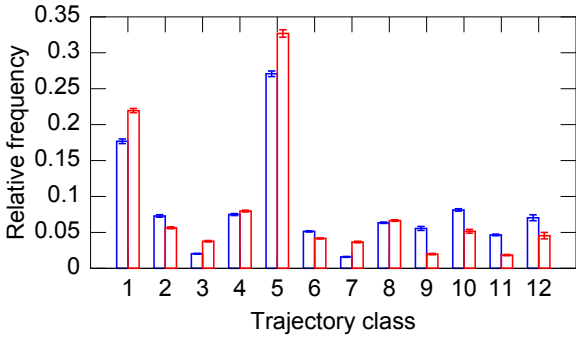

Fig. 12. Relative frequency of trajectory classes (blue = Sunday, red = Wednesday).

opposite end of the corridor (classes 1 and 5), were the most common. There is an observable difference between Sunday and Wednesday for the last four classes, suggesting that the square area is used more often on Sunday.

We observed very little variation in the frequencies of trajectory classes from day to day. However, changes can be observed during the day. Figure 13 shows the changes in the relative frequency of the classes, where we bound together classes explaining the movement towards the west (i.e. into the area), towards the east (out of the area), and the last 4 classes which include the activities on the square.

In the morning the trajectories going from east to west dominate, showing that there is a flow into the space. This is reversed in the late afternoon when the space gradually empties. In the Wednesday data the movements around lunch hour are apparent—there is first a flow going toward the east part of the shopping center, where most restaurants are located, and than back into the space. Even the Sunday data show a slightly higher flow towards the east between 12:00 and 13:00, which could also be explained by the lunch.

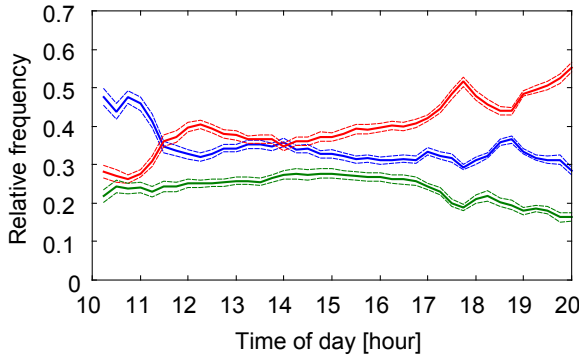

(a) Sunday

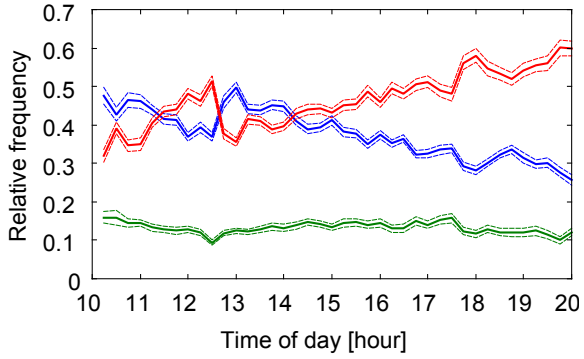

(b) Wednesday

Fig. 13. Relative frequency of trajectory classes during the day (blue = classes 1-4, red = classes 5-8, green = classes 9-12). The dashed lines show the ± 1 standard error.

VI. Model Based Data Fitting

A. Overview

There exist variations in the macroscopic pedestrian behavior, and inspection of the data seems to suggest factors like events and vacation days correlate with the changes. Here we fit a model to the data in order to show that it is possible to use a model for predicting the state of the environment, and to determine which factors are relevant for the model.

We will consider only the estimation of the number of people. We use a two step procedure, where we first learn a model for the average number of people for one day and than use the output of that model to predict the number of people during the day.

For modeling the nonlinear relationships we used a Gaussian process (GP) model [33]. A Gaussian process is in essence a random process in which every point and combinations of points have a normal distribution. The model is fully described by two functions, one for the mean and one for the covariance of the underlying distribution, and by adjusting the parameters of these functions it is possible to match the data. For all models we chose a mean function equal to zero and the so called squared exponential with automatic relevance determination [33] for the covariance function:

$$k(\mathbf{x}_p, \mathbf{x}_q) = \sigma^2 exp\left(-\frac{1}{2}\sum_{i=1}^{m}\frac{(x_{p,i}-x_{q,i})^2}{l_i}\right), \qquad (1)$$

where σ and l_i are the parameters of the covariance function, i.e. hyperparameters of the Gaussian process. The learning consists of finding the hyperparameters that give the best fit of the process to the data.

A convenient property of this model is "automatic relevance determination"—it automatically decreases the effect of the inputs not relevant for the estimate. This is encoded in the "length-scales" l_i: from (1) if after training l_i becomes much larger than the range of the input i, the covariance function will be practically unaffected by that input. For the computations we used the *gplm toolbox* [33].

B. Estimating the Average Number of People in a Day

We wish to estimate the average number of people during the observation period, Fig. 6. We separately estimate the values for Sunday and Wednesday.

As inputs we used variables identified in the analysis in section IV-B. For Sundays these were the events in the area and the vacation periods, both marked in Fig. 6(a). In addition we also use an input for the weather. Vacation input was coded with 1 during the vacation periods and 0 otherwise. Event input was encoded with 1 for days with events and 0 otherwise. The information on the events was available on the

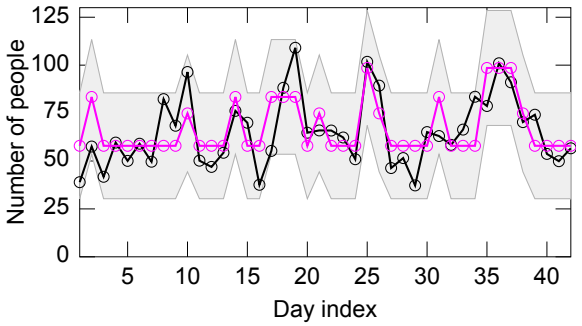

(a) Sunday

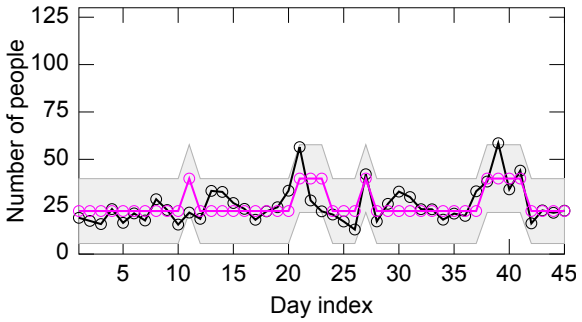

(b) Wednesday

Fig. 14. Modeling of the number of people in the whole space (black = original data, magenta = estimate). The gray area shows the 2 s.d. confidence region.

center's web page. Weather index input ranged from 1 (sunny) to 4 (heavy rain), parsed from Japan meteorological agency records. On Wednesdays there were no events, so we only used vacation and weather inputs. The one holiday which fell on a Wednesday was treated as a vacation day. (Even though the Gaussian process is defined on a continuous input space, the inputs have discrete values, so we look at the model output only for the specific input values.)

In order to evaluate the obtained GP model, we divided the input data into training and validation sets. Every third day from the dataset was chosen as the validation data, whereas the rest were used for training.

After learning the model, the hyperparameters showed that the weather index had only a very small effect on the estimate: length-scale ($l_{weather}$) was larger than 50 for the Sunday and Wednesday data. On the other hand, the length-scales for other inputs were smaller than 1. Therefore, we repeated the learning without the weather input.

The result of the estimation for the whole area data is shown in Fig. 14. The grayed area around the estimate shows the 2-standard-deviations confidence region, obtained from the covariance function of the underlying Gaussian process. The estimate appears to model most of the large trends in the data, although on some days the estimation error is larger than on others, suggesting that events and vacations do not capture all the changes.

Table I presents the obtained estimation errors. The error values for the estimated number of people in the whole area, corridor and square are shown. It shows that the GP model performs well both on the test as well as validation data.

For comparison we estimated the number of people on a specific day based on the observed number of people up to that day. A first order low-pass filter was used:

$$n_{filt}(i) = \alpha n_{filt}(i-1) + (1-\alpha)n(i), \qquad (2)$$

where $n(i)$ and $n_{filt}(i)$ are the observed and filtered number of people on day i, respectively. For all cases the factor α was set to 0.85, which was determined to give the best estimate. The filtered value was then used as an estimate of the number of people on the next day. The estimation errors using the filtered values are shown in Table I. In all cases the GP model yielded better performance.

TABLE I
ROOT MEAN SQUARED ERROR (RMSE) FOR THE ESTIMATION OF NUMBER OF PEOPLE THROUGH THE YEAR

		GP model		
Area	Day	Training	Validation	Filter
Whole	Wed	8.1	6.4	11.8
	Sun	12.8	15.6	21.8
Corridor	Wed	2.4	1.6	3.1
	Sun	4.1	4.2	5.1
Square	Wed	0.72	0.82	0.99
	Sun	3.0	1.4	5.6

C. Estimating the Variation During One Day

Next, we modeled the changes during the day, as shown in Fig. 8. In addition to the estimate of the average number of people for that day obtained in the previous section, we also used the hour of the day as input. Again, every third day in the full set was used for validation and the rest for training.

Fig. 15 shows the estimation results with and without vacation for Wednesdays and with and without events for Sundays that are not vacations. As compared to the original data with the same conditions, the model captures the main trends in the number of people.

Inspecting the original data there are large variations, especially for the Sunday data. Even on a single day the number of people can change considerably in a short time, possibly due to happenings outside of the tracking area. For example, in Fig. 15(a) two of the days show a large number of people in the morning. On both days there was a boat cruise that left from the ferry terminal west of the square, with people gathering in the area. Cruises happen rarely and this information is not on the center's website. The prominent peak in the afternoon on one Wednesday in Fig. 15(c), is also related to an event of the ferry company.

The training and validation error values are listed in Table II. As a comparison we trained a GP model using only time of day as input ("Only TOD" in the table). The model which considered events and vacations yields improved performance over the Only TOD model.

Finally, we also compared with an estimator based on the filtered value of previous days. The filtering is done for each interval (i.e. for each time-of-day value) separately using (2). The GP model outperforms this simple estimator.

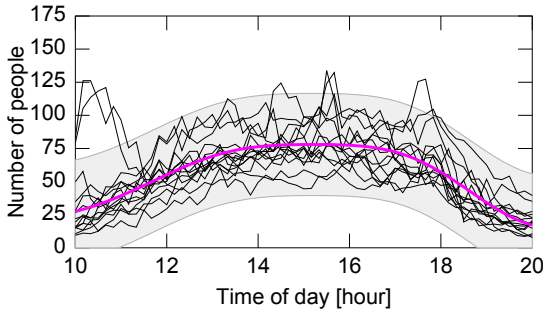

(a) Sunday - no event, no vacation

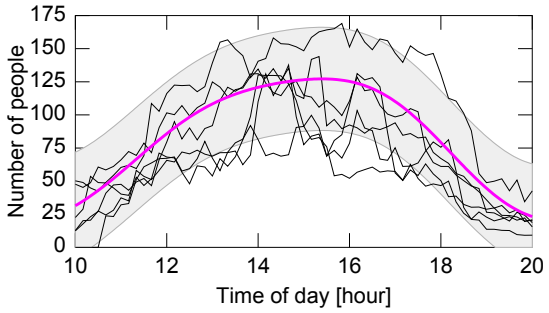

(b) Sunday - event, no vacation

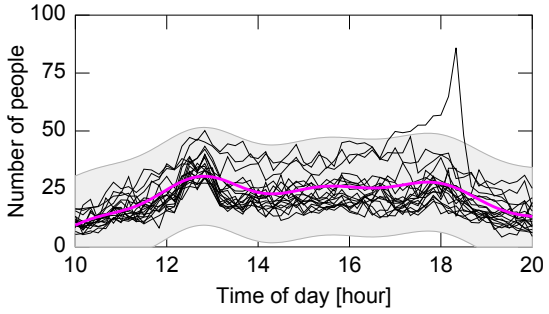

(c) Wednesday - no vacation

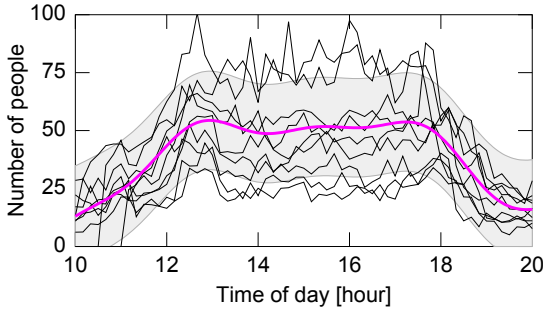

(d) Wednesday - vacation

Fig. 15. Modeling of the number of people in the whole space during the day: model (magenta) compared with original data for several days (black). The 2 s.d. confidence region of the GP model is shown in gray.

D. On the Necessary Dataset Size

If we exclude the influence of events and vacations, the analysis above shows that the density and speed statistics did not change very significantly throughout the year. This brings up a question about the number of days needed to produce a model that can satisfactorily describe the statistics for the whole year.

The answer will be dependent on the environment, the problem in question, and the needed model accuracy, but for illustration purposes we examine the effect of the dataset size for our case study. We use a model with only the time-of-day as input, and repeat the same training and evaluation as above. The training datasets consisted of a number of consecutive days from the full dataset whereas the model error was evaluated on the remaining days. For a fixed number of days in the training set, we evaluated the root mean square error on all possible sets of consecutive days, and then calculated the mean value of the errors as well as the maximum (worst case) error. We varied the number of the training days to obtain the results in Table III.

As the number of days in the dataset increases, the average modeling error decreases. The worst case error can be large when the dataset is too small, but it steadily decreases with the increasing size of the dataset. This means that even if the choice of training days is not optimal, with a large enough dataset the model will give a fairly good approximation. For example for Sunday data, if we use a dataset of 4 days the worst modeling error will be less then 50% larger than the mean error for the same dataset size.

These results are reassuring as they show that even with smaller datasets, the obtained model of the statistics should be descriptive for large periods of time.

TABLE II
ROOT MEAN SQUARED ERROR (RMSE) VALUES FOR THE ESTIMATION OF NUMBER OF PEOPLE DURING THE DAY

		GP model			
Area	Day	Training	Validation	Only TOD	Filter
Whole	Wed.	10.5	8.3	13.5	14.2
	Sun.	19.1	23.7	25.5	27.8
Corridor	Wed.	3.1	2.4	3.6	3.8
	Sun.	5.5	6.1	6.2	6.7
Square	Wed.	1.2	1.2	1.4	1.4
	Sun.	5.2	7.4	7.5	8.0

TABLE III
MODELING USING SMALLER DATASETS: RMSE STATISTIC FOR VARYING NUMBER OF DAYS IN THE DATASET

days in	Wednesday		Sunday	
dataset	mean	max	mean	max
1	15.9	39.8	33.7	72.7
2	15.0	29.1	30.1	44.7
4	14.2	24.1	27.8	36.6
6	13.5	18.6	26.8	32.8
8	13.2	14.9	26.0	29.7

VII. CONCLUSION

We analyzed the changes in the long-term usage of space inside a large area of a shopping mall. We used a tracking system based on 3-D range sensors for continuous online tracking of all people. The data were collected over one year, and we analyzed variables of interest, including density and velocity, and their changes.

We found that there are differences in space usage from day to day as well as during the day. Two factors identified to have an influence were events which happened inside the area and school vacation days. No effect of weather was confirmed. We have modeled the data using a Gaussian process model and the results showed that knowledge about influencing factors supports an advanced model for predicting the state of the space.

While the specific details of the analysis presented here are valid only for the environment of the data collection, we believe they can be illustrative of the basic trends in the macroscopic space usage, especially for similar environments.

We make part of the collected dataset (including raw sensor data) available to other researchers at http://www.irc.atr.jp/crest2010_HRI/ATC_dataset (more data can be made available on motivated request).

VIII. Acknowledgement

We thank our colleagues involved in setting up of the tracking environment and data collection: Masahiro Shiomi, Tetsushi Ikeda, Kotaro Hayashi, Francesco Zanlungo, Hiroyuki Kidokoro, Chao Shi, Yoshitaka Suehiro, Takuya Kitade, and Hajime Iba. We are grateful to the staff of the Asia & Pacific Trade Center for their support.

References

[1] S. Hoogendoorn and W. Daamen, "Design assessment of Lisbon transfer stations using microscopic pedestrian simulation," *Computers in railways VIII. WIT Press, Southampton*, pp. 135–147, 2004.

[2] A. Schadschneider, W. Klingsch, H. Klüpfel, T. Kretz, C. Rogsch, and A. Seyfried, "Evacuation dynamics: Empirical results, modeling and applications," in *Extreme Environmental Events*. Springer, 2011, pp. 517–550.

[3] D. Helbing and A. Johansson, "Pedestrian, crowd and evacuation dynamics," in *Extreme Environmental Events*. Springer, 2011, pp. 697–716.

[4] H. M. Dee and S. A. Velastin, "How close are we to solving the problem of automated visual surveillance?" *Machine Vision and Applications*, vol. 19, no. 5-6, pp. 329–343, 2008.

[5] A. Panangadan, M. Matarić, and G. Sukhatme, "Detecting anomalous human interactions using laser range-finders," in *Proceedings. 2004 IEEE/RSJ International Conference on Intelligent Robots and Systems, 2004.(IROS 2004).*, vol. 3, 2004, pp. 2136–2141.

[6] M. Bennewitz, W. Burgard, G. Cielniak, and S. Thrun, "Learning motion patterns of people for compliant robot motion," *International Journal of Robotics Research*, vol. 24, no. 1, pp. 31–48, 2005.

[7] P. Trautman and A. Krause, "Unfreezing the robot: Navigation in dense, interacting crowds," in *2010 IEEE/RSJ International Conference on Intelligent Robots and Systems (IROS)*, 2010, pp. 797–803.

[8] S. Satake, T. Kanda, D. F. Glas, M. Imai, H. Ishiguro, and N. Hagita, "How to approach humans?-strategies for social robots to initiate interaction," in *4th ACM/IEEE International Conference on Human-Robot Interaction (HRI)*, 2009, pp. 109–116.

[9] H. Kidokoro, T. Kanda, D. Brščić, and M. Shiomi, "Will I bother here?-a robot anticipating its influence on pedestrian walking comfort," in *8th ACM/IEEE International Conference on Human-Robot Interaction (HRI)*, 2013, pp. 259–266.

[10] T. Kitade, S. Satake, T. Kanda, and M. Imai, "Understanding suitable locations for waiting," in *8th ACM/IEEE International Conference on Human-Robot Interaction (HRI)*, 2013, pp. 57–64.

[11] D. Bauer, N. Brandle, S. Seer, M. Ray, and K. Kitazawa, "Measurement of pedestrian movements: A comparative study on various existing systems," in *Pedestrian Behavior: Models, Data Collection and Applications*, H. Timmermans, Ed. Emerald Group Publishing, 2009, pp. 325–344.

[12] B. Hillier, M. D. Major, J. Desyllas, K. Karimi, B. Campos, and T. Stonor, "Tate Gallery, Millbank: A study of the existing layout and new masterplan proposal," Bartlett School of Graduate Studies, University College London, Tech. Rep., 1996.

[13] J. S. Larson, E. T. Bradlow, and P. S. Fader, "An exploratory look at supermarket shopping paths," *International Journal of Research in Marketing*, vol. 22, no. 4, pp. 395–414, 2005.

[14] T. Kanda, M. Shiomi, L. Perrin, T. Nomura, H. Ishiguro, and N. Hagita, "Analysis of people trajectories with ubiquitous sensors in a science museum," in *IEEE International Conference on Robotics and Automation (ICRA)*, 2007, pp. 4846–4853.

[15] L. Aultman-Hall, D. Lane, and R. R. Lambert, "Assessing impact of weather and season on pedestrian traffic volumes," *Transportation Research Record: Journal of the Transportation Research Board*, vol. 2140, no. 1, pp. 35–43, 2009.

[16] C. Stauffer and W. E. L. Grimson, "Learning patterns of activity using real-time tracking," *IEEE Transactions on Pattern Analysis and Machine Intelligence*, vol. 22, no. 8, pp. 747–757, 2000.

[17] D. Ellis, E. Sommerlade, and I. Reid, "Modelling pedestrian trajectory patterns with gaussian processes," in *IEEE 12th International Conference on Computer Vision Workshops*, 2009, pp. 1229–1234.

[18] X. Wang, K. T. Ma, G.-W. Ng, and W. E. L. Grimson, "Trajectory analysis and semantic region modeling using nonparametric hierarchical bayesian models," *International Journal on Computer Vision*, vol. 95, no. 3, pp. 287–312, 2011.

[19] S. Pellegrini, A. Ess, K. Schindler, and L. Van Gool, "You'll never walk alone: Modeling social behavior for multi-target tracking," in *2009 IEEE 12th International Conference on Computer Vision*, 2009, pp. 261–268.

[20] H. Zhao and R. Shibasaki, "A novel system for tracking pedestrians using multiple single-row laser-range scanners," *IEEE Transactions On Systems, Man and Cybernetics, A*, vol. 35, no. 2, pp. 283–291, 2005.

[21] D. Glas, T. Miyashita, H. Ishiguro, and N. Hagita, "Laser-based tracking of human position and orientation using parametric shape modeling," *Advanced Robotics*, vol. 23, no. 4, pp. 405–428, 2009.

[22] L. Navarro-Serment, C. Mertz, and M. Hebert, "Pedestrian detection and tracking using three-dimensional ladar data," in *Proceedings of the 7th International Conference on Field and Service Robotics*, Cambridge, MA, USA, Jul. 2009.

[23] L. Spinello, M. Luber, and K. Arras, "Tracking people in 3D using a bottom-up top-down detector," in *Proceedings of the IEEE International Conference on Robotics and Automation (ICRA'11)*, Shanghai, China, May 2011, pp. 1304–1310.

[24] D. Brščić, T. Kanda, T. Ikeda, and T. Miyashita, "Person tracking in large public spaces using 3-D range sensors," *IEEE Transactions on Human-Machine Systems*, vol. 43, no. 6, pp. 522–534, 2013.

[25] M. Nikolić, B. Farooq, and M. Bierlaire, "Exploratory analysis of pedestrian flow characteristics in mobility hubs using trajectory data," in *13th Swiss Transport Research Conference*, 2013.

[26] D. Helbing and P. Molnar, "Social force model for pedestrian dynamics," *Physical review E*, vol. 51, no. 5, p. 4282, 1995.

[27] F. Zanlungo, T. Ikeda, and T. Kanda, "Social force model with explicit collision prediction," *EPL (Europhysics Letters)*, vol. 93, no. 6, p. 68005, 2011.

[28] S. J. Guy, J. Chhugani, S. Curtis, P. Dubey, M. Lin, and D. Manocha, "Pledestrians: a least-effort approach to crowd simulation," in *Proceedings of the 2010 ACM SIGGRAPH/Eurographics Symposium on Computer Animation*. Eurographics Association, 2010, pp. 119–128.

[29] B. Morris and M. Trivedi, "A survey of vision-based trajectory learning and analysis for surveillance," *IEEE Transactions on Circuits and Systems for Video Technology*, vol. 18, no. 8, pp. 1114–1127, 2008.

[30] D. Vasquez, T. Fraichard, and C. Laugier, "Growing hidden markov models: An incremental tool for learning and predicting human and vehicle motion," *The International Journal of Robotics Research*, vol. 28, no. 11-12, pp. 1486–1506, 2009.

[31] B. Keni and S. Rainer, "Evaluating multiple object tracking performance: the CLEAR MOT metrics," *EURASIP Journal on Image and Video Processing*, vol. 2008, 2008.

[32] L. Kaufman and P. J. Rousseeuw, *Finding groups in data: an introduction to cluster analysis*. Wiley.com, 2009, vol. 344.

[33] C. E. Rasmussen and C. K. I. Williams, *Gaussian Processes for Machine Learning (Adaptive Computation and Machine Learning)*. The MIT Press, 2005.

Dražen Brščić (S'06-M'09) received his B.Sc. and M.Sc. degrees in electrical engineering from the University of Zagreb, Croatia, in 2000 and 2004, respectively, and the Dr.Eng. degree in electrical engineering from The University of Tokyo, Japan in 2008. From 2008 to 2010 he worked as a post-doctoral researcher at the Technische Universität München, Germany. In 2011 he joined ATR Intelligent Robotics and Communication Laboratories in Kyoto, Japan, as research scientist. His research interests include person tracking, mobile robotics and human-robot interaction.

Takayuki Kanda (M'04) received the B.Eng, M.Eng, and Ph.D. degrees in computer science from Kyoto University, Kyoto, Japan, in 1998, 2000, and 2003, respectively. From 2000 to 2003, he was an Intern Researcher with the Advanced Telecommunications Research Institute International (ATR) Media Information Science Laboratories. He is currently a Senior Researcher with the ATR Intelligent Robotics and Communication Laboratories, Kyoto, Japan. His research interests include intelligent robotics, humanrobot interaction, and vision-based mobile robots. Dr. Kanda is a member of the Association for Computing Machinery, the Robotics Society of Japan, and the Information Processing Society of Japan.